Photoproduction off nuclei and pointlike photon interactions. I. Cross sections and nuclear shadowing

R. Engel
Universität Leipzig, Fachbereich Physik, D-04109 Leipzig, Germany
and Universität Siegen, Fachbereich Physik, D-57068 Siegen, Germany

J. Ranft*
Departamento de Física de Partículas, Universidade de Santiago de Compostela, E-15706 Santiago de Compostela, Spain

S. Roesler
Universität Siegen, Fachbereich Physik, D-57068 Siegen, Germany
(Received 9 October 1996)

High energy photoproduction off nuclear targets is studied within the Glauber-Gribov approximation. The photon is assumed to interact as a $q\overline{q}$ system according to the generalized vector dominance model and as a ''bare photon'' in direct scattering processes with target nucleons. We calculate total cross sections for interactions of photons with nuclei taking into account coherence length effects and pointlike interactions of the photon. Results are compared to data on photon-nucleus cross sections, nuclear shadowing, and quasielastic ρ production. Extrapolations of cross sections and of the shadowing behavior to high energies are given. [S0556-2821(97)06511-9]

PACS number(s): 12.40.Vv, 13.60.Hb

I. INTRODUCTION

During the last years, the understanding of photon-hadron interactions has considerably improved due to new experimental data from photoproduction and low-x measurements in ep collisions at the DESY ep collider HERA and due to their interpretation in terms of QCD-inspired multiple-interaction models [1]. Experimental evidence for the classification of photon interactions within the parton model into *direct* and *resolved* interactions has been found [2–4]. Both classes of processes show different features concerning cross sections as well as multiparticle production [2,5,6].

Within the QCD-improved parton model, in direct processes the photon couples directly to a parton of the hadron, whereas in resolved processes it enters the scattering process as a hadronic quark-antiquark fluctuation. Resolved processes are well described using the QCD-improved parton model (recent reviews are given in [7,8]) and the generalized vector dominance model (GVDM) (see for example [9,10] and references therein). Because of relatively large lifetimes, the $q\overline{q}$ states may develop properties of ordinary hadrons by emitting and absorbing virtual partons. Therefore, the $q\overline{q}$ states can either interact with the hadron in soft scattering processes (the produced final-state particles have small transverse momenta) or the partons of the $q\overline{q}$ system can participate in hard interactions with the partons of the hadron [11]. In case of a hard interaction, and if the mass of the $q\overline{q}$ fluctuation is large in comparison to the perturbative QCD scale Λ_{QCD}, it is possible to calculate not only the hard parton-parton scattering but also the splitting of the photon into the $q\overline{q}$ pair perturbatively. These hard resolved interactions of high-mass $q\overline{q}$ states are frequently called *anomalous* photon interactions [12].

Here, we want to study the implications of the above mentioned experimental findings on direct and resolved processes to the understanding of photon-nucleus collisions at comparable or higher photon energies.

High energy photon-nucleus collisions have been studied experimentally and theoretically by numerous groups (for recent reviews we refer to [13,14]). It was found that they bear a remarkable resemblance to hadron-nucleus interactions. For instance, both show decreasing per-nucleon cross sections with increasing nucleus mass number, an effect which is known as ''shadowing.'' Again, the GVDM provides a natural interpretation of these photon-hadron similarities [9,15]. Like in hadron-nucleus collisions, shadowing in photon-nucleus collisions can then be described in the framework of the Gribov-Glauber approximation [16–18]. It relates the total photon-nucleus cross section to effective $q\overline{q}$-nucleon cross sections [14,19–22]. However, the application of the Gribov-Glauber formalism to the multiple scattering process of a $q\overline{q}$ state without further constraints is only justified if the interaction length exceeds the nuclear radius [23]. This is not the case for the above mentioned direct processes since the photon interacts in such processes with only one nucleon. As we will further argue below, at high energies it might also be not the case for anomalous photon interactions. In particular, we will consider the extreme assumption that the interaction time is less than any internucleon distance, i.e., that again only one target nucleon is involved. For these reasons, in the following we call direct and anomalous photon interactions *pointlike* processes. They may lead to a suppression of the Glauber-multiple scattering process, i.e., to a suppression of shadowing. It can be expected that this feature is most clearly pronounced in photon

*Present address: INFN-Laboratori Nationali del Gran Sasso, I-67010 Assergi AQ, Italy.

scattering processes off heavy nuclei and at high energies, where the cross section of the pointlike photon-nucleon interaction becomes sizable as compared to the total photon-nucleon cross section.

The intention of the present paper is twofold: calculating cross sections of photon-nucleus interactions, we (i) investigate the influence of pointlike processes on the shadowing behavior at high energies, and (ii) provide the basis for a study of particle production in photon-nucleus collisions [24]. In Sec. II we consider photon-nucleon collisions and derive total cross sections for $q\bar{q}$-nucleon interactions. In Sec. III pointlike photon interactions are discussed and their contribution to the total photon-nucleon cross section is estimated. In Sec. IV we calculate photon-nucleus cross sections and the shadowing behavior. Both are compared to data on photoproduction and deep inelastic scattering (DIS) off nuclei and extrapolations to high energies are given. Finally, in Sec. V we summarize our results.

II. TOTAL PHOTON-NUCLEON CROSS SECTIONS

Throughout this paper we consider the photon-nucleon scattering process in the laboratory frame (nucleon rest frame) using the following kinematical variables. The Bjorken-x variable is defined as $x=Q^2/2m\nu$ denoting with Q^2, ν, and m the photon virtuality, the photon energy, and the nucleon mass, respectively. The squared total energy of the photon-nucleon system is given by $s=Q^2(1-x)/x+m^2$. We restrict our discussions to small x values ($x<0.1$) and to the limit $s\gg Q^2$.

Within the diagonal GVDM [9,10] it is assumed that the virtual photon fluctuates into intermediate $q\bar{q}$ states V of mass M which subsequently may interact with the nucleon N. This fact can be expressed by a spectral relation of the form [15,14,25]

$$\sigma_{\gamma^\star N}(s,Q^2)=4\pi\alpha_{\rm em}\int_{M_0^2}^{M_1^2}dM^2D(M^2)\left(\frac{M^2}{M^2+Q^2}\right)^2 \times\left(1+\epsilon\frac{Q^2}{M^2}\right)\sigma_{VN}(s,Q^2,M^2). \quad (1)$$

We use $\alpha_{\rm em}=e^2/4\pi=1/137$. The factor $D(M^2)$ incorporates the density of $q\bar{q}$ systems per unit mass-squared interval:

$$D(M^2)=\frac{R_{e^+e^-}(M^2)}{12\pi^2M^2},$$

$$R_{e^+e^-}(M^2)=\frac{\sigma_{e^+e^-\to\text{hadrons}}(M^2)}{\sigma_{e^+e^-\to\mu^+\mu^-}(M^2)}\approx 3\sum_f e_f^2, \quad (2)$$

where we sum up the squared quark charges of all quark flavors being energetically accessible. ϵ is the ratio between the fluxes of longitudinally and transversally polarized photons. σ_{VN} denotes the effective cross section for the interaction of a $q\bar{q}$ system with mass M with a nucleon.

Considering low-Q^2 $\gamma^\star p$ scattering only, a detailed model for the M^2 and Q^2 dependence of σ_{VN} is not needed. At high collision energies, the average lifetime of the hadronic $q\bar{q}$ fluctuation $t_f\sim 2\nu/(M^2+Q^2)$ is almost always larger than the typical hadronic interaction time $t_{\rm int}$ (for nucleons $t_{\rm int}\sim r_N\approx 1$ fm). However, in photon-nucleus collisions the M^2 and Q^2 dependence of σ_{VN} might be important since the coherence length $d\sim t_f$ of the hadronic fluctuation can become comparable to or smaller than the nuclear radius or the nuclear mean free path [$\approx 1/(n\sigma_{VN})$, with n being the number of nucleons per unit volume] [15]. Therefore, in the following we are going to estimate the (purely theoretical) quantity σ_{VN} using Eq. (1) and a parametrization for the experimentally measurable cross section $\sigma_{\gamma^\star N}$.

With increasing mass M of the $q\bar{q}$ system the virtuality of the q and $\bar{q}$ of the system increases. As a consequence, the transverse size of the hadronic fluctuation and, hence, σ_{VN} decreases like $1/M^2$ at large M^2 [15,22]. Following Ref. [15] we approximate this effect parametrizing σ_{VN} as

$$\sigma_{VN}(s,Q^2,M^2)=\frac{\tilde{\sigma}_{VN}(s,Q^2)}{M^2+Q^2+C^2}. \quad (3)$$

Here, C is a model-dependent parameter [15] and taken to be $C^2=2$ GeV^2. With Eq. (3) the M^2 dependence of the integrand in Eq. (1) is explicitly known and the integration over M^2 between $M_0^2=4m_\pi^2$ and $M_1^2=s$ can be performed. The lower integration limit corresponds to the kinematical threshold. Alternatively, the contributions from the low mass vector mesons ρ^0, ω, and ϕ could be added as separate terms to the continuum [Eq. (1)], in this case starting the integration at m_ϕ^2 [14,26]. However, this has been omitted for simplicity. The upper limit, here formally taken to be s, has practically no influence on the results at low and moderate Q^2 since high M^2 values are suppressed. The only quantity on the right hand side (RHS) of Eqs. (1) and (3) which is unknown so far is $\tilde{\sigma}_{VN}$. Using a parametrization for $\sigma_{\gamma^\star N}$, the M^2 independent part of Eq. (3), $\tilde{\sigma}_{VN}$, can be calculated for each value of s and Q^2.

Applying the convention of Ref. [27], the cross section for the scattering of virtual photons off nucleons $\sigma_{\gamma^\star N}$ can be written as

$$\sigma_{\gamma^\star N}(s,Q^2)=\frac{4\pi^2\alpha_{\rm em}}{Q^2(1-x)}F_2^N(x,Q^2). \quad (4)$$

Since in the present paper we want to study cross sections and shadowing in the Q^2 region of both, photoproduction and DIS, we use the model of Capella, Kaidalov, Merino, and Trân Thanh Vân [28] (CKMT) for the structure function F_2^N which provides a simple analytical parametrization valid for $0\leqslant Q^2\lesssim 5$ GeV^2. The nucleon structure function is derived from Regge arguments taking rescattering effects into account:

$$F_2^N(x,Q^2)=Ax^{-\Delta(Q^2)}(1-x)^{n(Q^2)+4}\left(\frac{Q^2}{Q^2+a}\right)^{1+\Delta(Q^2)} + Bx^{1-\alpha_R}(1-x)^{n(Q^2)}\left(\frac{Q^2}{Q^2+b}\right)^{\alpha_R} \quad (5)$$

with

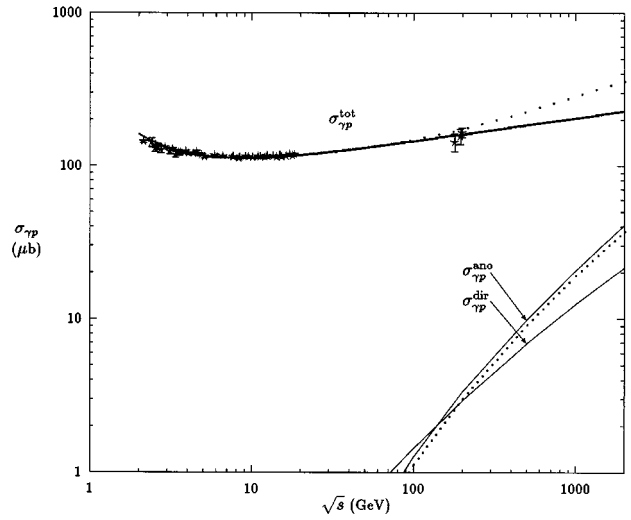

FIG. 1. Total photon-proton cross sections as calculated with the CKMT model [28] (thick solid line) and obtained within the two-component DPM (dotted line) are shown together with measurements [33–35]. In addition, we give the contribution to the total cross section from direct processes and the cross section reflecting the anomalous component of the photon-PDFs. The latter are calculated using the GRV [44,45] (solid line) and SaS-2D [47] (dotted line) PDF parametrizations.

$$\Delta(Q^2)=\Delta_0\left(1+\frac{2Q^2}{Q^2+d}\right), \quad n(Q^2)=\frac{3}{2}\left(1+\frac{Q^2}{Q^2+c}\right). \tag{6}$$

The first term in Eq. (5) is associated with the pomeron contribution determining the small-x behavior of the sea-quark distribution function, whereas the second term is parametrized according to secondary reggeon contributions governing the valence-quark distribution function of the nucleon. We refer to [28] for the values of the parameters entering the expressions. The structure function resulting from this model is in reasonable agreement with measurements [28]. Using the ansatz for the gluon distribution as given in [28] we obtain F_2^N for higher values of Q^2 by performing a QCD evolution in leading logarithmic approximation.

We note that also other parametrizations would be suitable, for instance the parametrization of Abramowicz *et al.* [29] and in the low Q^2 range the parametrizations of Badelek and Kwieciński [30]. Furthermore, for low values of Q^2 the photon-nucleon cross section $\sigma_{\gamma^\star N}$ can be equally well obtained in the framework of the two-component dual parton model (DPM) [31,32]. The advantage of the two-component DPM calculation is that in this case a detailed model for the inelastic final states exists [32], which is also applied to the study of particle production in [24].

In Fig. 1 we compare the photoproduction cross sections $\sigma^{\rm tot}_{\gamma p}$ obtained from the CKMT model (thick solid line) and calculated within the two-component DPM (dotted line) with data [33–35]. The differences in the high energy extrapolation reflect the typical size of the theoretical uncertainties.

In Fig. 2(a) we show the energy-dependence of the effective cross section σ_{VN} for $M^2=m_\rho^2$ and different Q^2 values. As observed in $\gamma^\star p$ collisions, the rise of the cross section with energy becomes steeper with increasing photon virtuality. In Fig. 2(b) the Q^2 dependence of σ_{VN} for different energies and $M^2=m_\rho^2$ is given. As expected, the Q^2 dependence is very weak for $Q^2<m_\rho^2+C^2$.

III. CONTRIBUTIONS FROM POINTLIKE INTERACTIONS OF THE PHOTON

The integral in Eq. (1) receives also contributions from hadronic fluctuations with large mass M. In terms of the QCD-improved parton model the hadronic interactions of these high-mass fluctuations ($q\overline{q}$ states) correspond to pointlike photon interactions. The average transverse momentum of the partons of such a $q\overline{q}$ state is proportional to its mass [22]. Hence, on this basis direct and resolved photon interactions are included in Eq. (1). Of course, a sharp distinction between direct and resolved interactions is not possible. In direct interactions, the photon couples directly to a parton of the nucleon which determines the highest virtuality of the scattering process [see Fig. 3(a)]. In resolved interactions, the photon may fluctuate into a $q\overline{q}$ pair with high virtuality. For example, a $q\overline{q}$ system can emit a gluon leading to a quark with even higher virtuality which couples to a gluon of

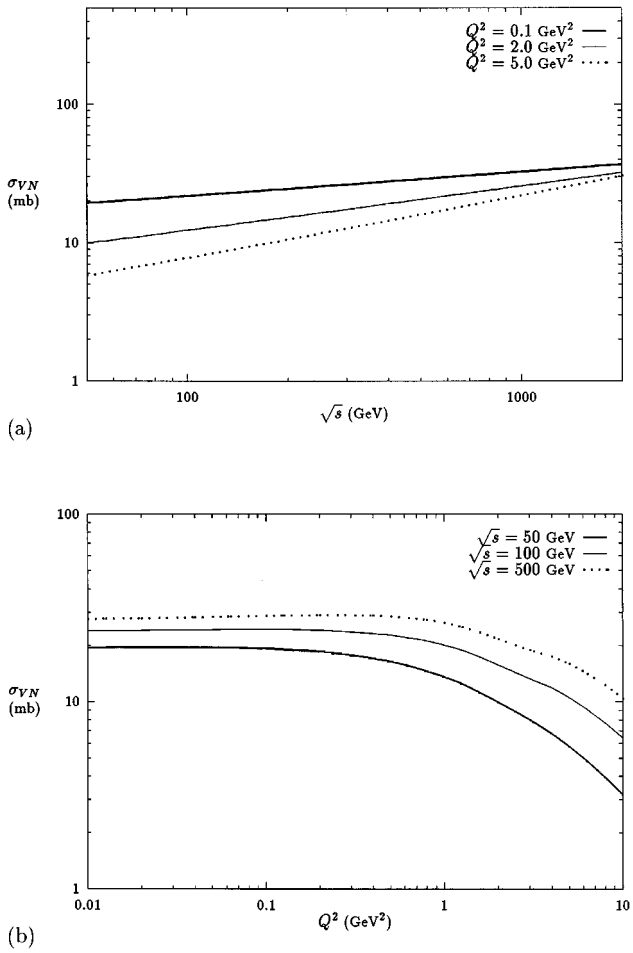

FIG. 2. The effective $q\overline{q}$-nucleon cross sections at $M^2=m_\rho^2$ are shown. In (a) the dependence on the energy is given for three different photon virtualities. In (b) we show the Q^2-behavior for three different energies.

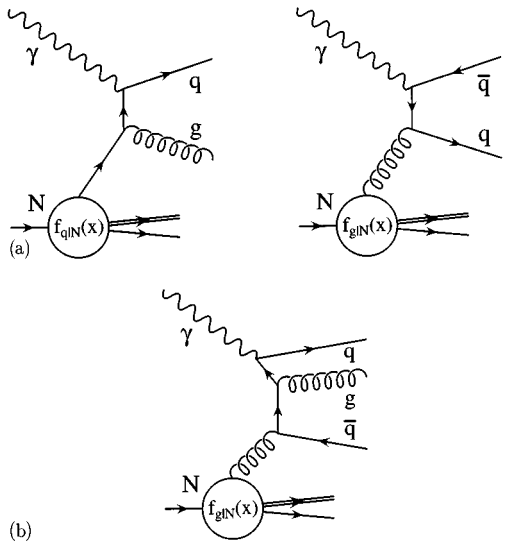

FIG. 3. Examples for pointlike interactions of the photon. In (a) direct photon-nucleon interactions contributing in lowest order pQCD and in (b) an example for an anomalous photon-nucleon interaction are shown.

the nucleon as shown in Fig. 3(b). Therefore, it is necessary to distinguish two scales to characterize a hard photon-nucleon scattering: (i) the virtuality M of the hadronic $q\overline{q}$ fluctuation and (ii) the scale of the hard scattering μ, which is approximately given by the momentum transfer in the hard scattering process. Then, for $\mu^2 \approx M^2$ the interaction is classified as direct interaction whereas for $\mu^2 \gg M^2$ the interaction is a resolved one. As already mentioned, in case of resolved interactions with $\mu^2 \gg M^2$ and $M^2 \gg \Lambda^2_{\rm QCD}$, not only the hard parton-parton scattering but also the splitting of the photon into the $q\overline{q}$ pair can be calculated perturbatively. These interactions lead to a rise of the photon structure function with μ^2 like $\ln(\mu^2)$ [36] (anomalous contribution to the photon structure function [12]). In the following we consider as pointlike photon interactions all processes which are characterized by $M^2 \gg \Lambda^2_{\rm QCD}$.

In direct and anomalous processes either M^2 or the transverse momentum of the hard scattering, $p_\perp$, acts as hard scale permitting perturbative calculations. Therefore, the cross section for direct processes $\sigma^{\rm dir}_{\gamma^\star N}$ and the cross section $\sigma^{\rm ano}_{\gamma^\star N}$ for the fluctuation of a photon into a $q\overline{q}$ system with a large mass M (i.e., highly virtual quarks) and the interaction of this system with a nucleon can be estimated using perturbative QCD.

In lowest-order perturbative QCD, the direct photon-nucleon cross section follows from

$$\sigma^{\rm dir}_{\gamma^\star N}(s,p_\perp^{\rm cutoff}) = \int dx d\hat{t} \sum_{i,k,l} f_{i|N}(x,\mu^2) \times \frac{d\sigma^{\rm QCD}_{\gamma,i\to k,l}(\hat{s},\hat{t})}{d\hat{t}} \Theta(p_\perp - p_\perp^{\rm cutoff}), \quad (7)$$

where $f_{i|N}$ denotes the parton distribution function (PDF) for the parton i of the nucleon and the sum runs over all possible parton configurations (i,k,l). For the calculation we use $\mu^2 = p_\perp^2/4$. The transverse momentum cutoff $p_\perp^{\rm cutoff}$ restricts the integration to the perturbatively reliable region.

In order to calculate the anomalous cross section $\sigma^{\rm ano}_{\gamma^\star N}$, we use the PHOJET Monte Carlo (MC) event generator [31,32] to simulate hard resolved photon-nucleon interactions according to the cross section

$$\sigma^{\rm res}_{\gamma N}(s,p_\perp^{\rm cutoff}) = \int dx_1 dx_2 d\hat{t} \sum_{i,j,k,l} \left(\frac{1}{1+\partial_{k,l}} \times f_{i|\gamma}(x_1,\mu^2) f_{j|N}(x_2,\mu^2) \times \frac{d\sigma^{\rm QCD}_{i,j\to k,l}(\hat{s},\hat{t})}{d\hat{t}} \Theta(p_\perp - p_\perp^{\rm cutoff}) \right). \quad (8)$$

This cross section receives contributions from low-mass and high-mass $q\overline{q}$ fluctuations. In order to determine the cross section due to anomalous interactions, initial state parton showers were generated for each hard interaction using a backwards evolution algorithm similar to the one discussed in [37,38] using the parton transverse momentum as evolution variable. Some basic coherence effects are implemented by imposing angular ordering of the parton emissions. Furthermore, the possibility to have a hard $\gamma \to q\overline{q}$ process during the shower evolution is taken into account. After each parton emission, the probability to stop the parton shower evolution due to a pointlike splitting is taken to be the ratio of the $\gamma \to q\overline{q}$ contribution to the quark density in the photon

$$q(x,\mu^2) = \frac{3\alpha_{\rm em}}{2\pi} e_q^2 \left[[x^2 + (1-x)^2] \ln\left(\frac{1-x}{x} \frac{\mu^2}{(p_\perp^{\rm cutoff})^2} \right) + 8x(1-x) - 1 \right] \quad (9)$$

and the quark density of the full photon PDF. Since we are only interested in $\gamma \to q\overline{q}$ splittings with a remnant quark having $p_\perp > p_\perp^{\rm cutoff}$, the transverse momentum cutoff $p_\perp^{\rm cutoff}$ is used in Eq. (9) as the lowest quark virtuality. Then, the fraction of the anomalous cross section to the total hard resolved photon-nucleon cross section is given by the fraction of events where an anomalous splitting with $p_\perp > p_\perp^{\rm cutoff}$ has been generated. Within the calculations, we use the GRV PDF parametrization for the proton [39]. Recent HERA measurements showed that this parametrization gives a reasonable description of the proton structure function at low x [40,41]. We however note that also the CTEQ4 [42] and Martin-Roberts-Stirling set R [MRS(R)] [43] PDF's could be applied in this study since in the considered energy range the differences between all these PDF parametrizations are unimportant for our purpose. Concerning the photon structure function much less data are available. In the following we choose the GRV parametrization for the photon PDF's [44,45] which has been successfully applied to reproduce HERA measurements [1,46]. In order to estimate uncertainties of the calculations the SaS-2D parametrization [47] is used additionally. For the transverse momentum cutoff a value of 3 GeV/c is applied consistently to both, direct and resolved interactions. In [24] particle production in photon-nucleus interactions based on the PHOJET model for the de-

scription of photon-nucleon interactions is studied. There, we argue that a model which should give a reasonable description of photoproduction off nuclei has to be able to describe the main features of photon-proton interactions as well. Since it was found by the H1 Collaboration [5] that the PHOJET event generator provides a reasonable description of γp photoproduction at 200 GeV c.m. energy using a transverse momentum cutoff of 3 GeV/c we use this value consistently for the calculation of cross sections and of particle production in photon-proton and in photon-nucleus interactions. It should be emphasized that using a much lower transverse momentum cutoff, the strong parton virtuality ordering assumed in the parton model expression (8) becomes questionable since very small x-values would enter this equation [48]. The formalism presented here is only applicable for photons with low Q^2, i.e., $Q^2 \ll 4p_\perp^2$. In Fig. 1 the calculated cross sections for direct and anomalous photon interactions on a proton target are shown. In addition we plot the results from a calculation using the SaS-2D PDFs for the photon [47]. The differences between the results obtained with the two PDF parametrizations are small and do not change the qualitative conclusions drawn from this investigation.

IV. PHOTON-NUCLEUS INTERACTIONS

A. Cross sections

The application of Eq. (1) to the scattering of a virtual photon on a nuclear target of mass number A is straightforward (see [14] and references therein). In order to calculate the total virtual photon-nucleus cross section $\sigma_{\gamma^\star A}$, σ_{VN} has to be replaced by the effective cross section σ_{VA} for the interaction of a $q\overline{q}$ system of mass M with a nucleus with mass number A:

$$\sigma_{\gamma^\star A}(s,Q^2)=4\pi\alpha_{\rm em}\int_{M_0^2}^{M_1^2} dM^2 D(M^2)\left(\frac{M^2}{M^2+Q^2}\right)^2 \times\left(1+\epsilon\frac{Q^2}{M^2}\right)\sigma_{VA}(s,Q^2,M^2). \quad (10)$$

σ_{VA} is obtained as follows: For coherence lengths d of the hadronic fluctuation

$$d=\frac{2\nu}{M^2+Q^2} \quad (11)$$

exceeding the average distance between two nucleons the $q\overline{q}$ system may interact coherently with several nucleons of the target nucleus. This multiple scattering process can be described using the MC realization of the Glauber-Gribov approximation by Shmakov *et al.* [49], here, extended to photon projectiles. The high energy small-angle scattering amplitude F for the interaction of a $q\overline{q}$ system with a nucleus at impact parameter $\vec{b}$ can be written in terms of the impact parameter amplitude Γ for the interaction of the $q\overline{q}$ system with individual nucleons [49]

$$F(\vec{b})=\langle\psi_A^f|1-\prod_{i=1}^{A}[1-\Gamma(\vec{b}_i)]|\psi_A^i\rangle, \quad \vec{b}_i=\vec{b}-\vec{s}_i. \quad (12)$$

The $\vec{s}_i$ are the coordinates of the nucleons with regard to the center of mass of the nucleus in the plane of impact parameter. The scattering amplitude is averaged over the initial and final state wave functions ψ_A^i and ψ_A^f of the nucleus. For the $q\overline{q}$-nucleon scattering amplitude we assume the parametrization

$$\Gamma(s,Q^2,M^2,\vec{b})=\frac{\sigma_{VN}(s,Q^2,M^2)}{4\pi B(s,Q^2,M^2)} \times\left(1-i\frac{{\rm Re}f(0)}{{\rm Im}f(0)}\right)\exp\left(\frac{-\vec{b}^2}{2B(s,Q^2,M^2)}\right). \quad (13)$$

The effective $q\overline{q}$-nucleon cross section σ_{VN} is obtained as discussed in Sec. II [Eq. (3)]. We adopt the parametrization of the slope B from [50]

$$B(s,Q^2,M^2)=2\left[B_0^2+\alpha'_{\rm I\!P}\ln\left(\frac{s}{M^2+Q^2}\right)\right],$$

$$B_0^2=\left(2+\frac{m_\rho^2}{M^2+Q^2}\right){\rm GeV}^{-2}, \quad \alpha'_{\rm I\!P}=0.25{\rm GeV}^{-2}, \quad (14)$$

and assume for the ratio ${\rm Re}f(0)/{\rm Im}f(0)$ a constant value of 0.1. Neglecting correlations between nucleons one may write

$$|\psi_A^i|^2=\prod_{j=1}^{A}\rho_A(\vec{s}_j,z_j), \quad \rho_A(\vec{r})=\frac{K}{1+\exp[(|\vec{r}|-R_A)/c]} \quad (15)$$

where ρ_A is the one-particle Woods-Saxon density distribution with $c=0.545$ fm and $R_A=1.12A^{1/3}$ fm [51]. Therefore, for the total, inelastic, and elastic $q\overline{q}$-nucleus cross sections $\sigma_{VA}^{\rm tot}$, $\sigma_{VA}^{\rm inel}$, and $\sigma_{VA}^{\rm el}$ we obtain

$$\sigma_{VA}^{\rm tot}(s,Q^2,M^2)=2{\rm Re}\int d^2bF(s,Q^2,M^2,\vec{b}) =2{\rm Re}\left\{\int d^2b\int\prod_{j=1}^{A}d^3r_j\rho_A(\vec{r}_j) \times\left(1-\prod_{i=1}^{A}[1-\Gamma(s,Q^2,M^2,\vec{b}_i)]\right)\right\}, \quad (16)$$

$$\sigma_{VA}^{\rm inel}(s,Q^2,M^2)=\int d^2b(1-|1-F(s,Q^2,M^2,\vec{b})|^2) =\int d^2b\int\prod_{j=1}^{A}d^3r_j\rho_A(\vec{r}_j) \times\left(1-\left|\prod_{i=1}^{A}[1-\Gamma(s,Q^2,M^2,\vec{b}_i)]\right|^2\right), \quad (17)$$

$$\sigma_{VA}^{\rm el}(s,Q^2,M^2)=\sigma_{VA}^{\rm tot}(s,Q^2,M^2)-\sigma_{VA}^{\rm inel}(s,Q^2,M^2). \quad (18)$$

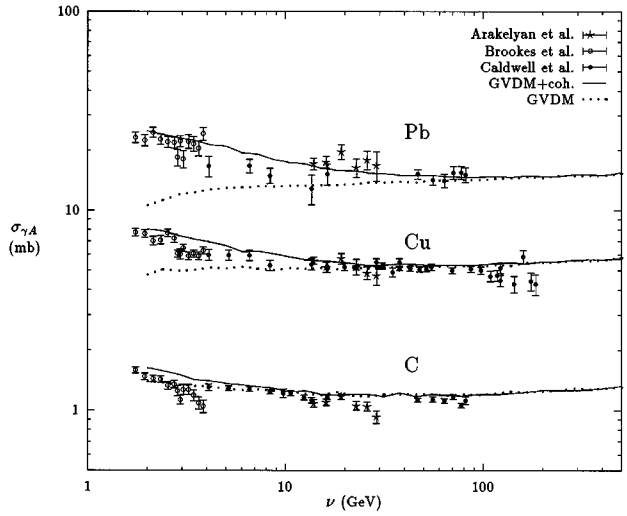

FIG. 4. The dependence of the total cross sections for interactions of real photons with carbon, copper, and lead on the photon energy (full lines) is compared to measurements [53–56]. The influence of the coherence length is indicated by dotted lines where we show the cross sections as they would be obtained disregarding the finite coherence length of the photon.

The integrations over the $\vec{r}_j$'s are performed by taking the average of the integrand in Eqs. (16), (17) over a sufficiently large number of nucleon coordinates sets sampled from the density distribution ρ_A.

At low energies the coherence length d may lead to a suppression of shadowing which we take into account in the calculation of the product over the A nucleons for a fixed spatial nucleon configuration [Eqs. (16), (17)]. In the nonshadowing limit, i.e., if d is smaller than any internucleon distance, we obtain a sum over $\Gamma(\vec{b}_i)$ and, therefore, $\sigma_{VA} \approx A\sigma_{VN}$.

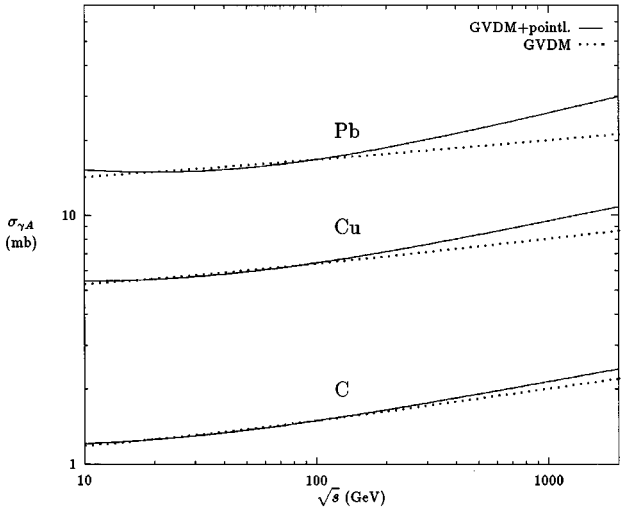

FIG. 5. Extrapolation of total cross sections for photoproduction off carbon-, copper-, and lead-nuclei. $\sqrt{s}$ is the photon-nucleon c.m. energy. The pure GVDM prediction is shown by the dotted lines. The cross sections taking the suppression of shadowing by pointlike photon-nucleon interactions into consideration are given by solid lines.

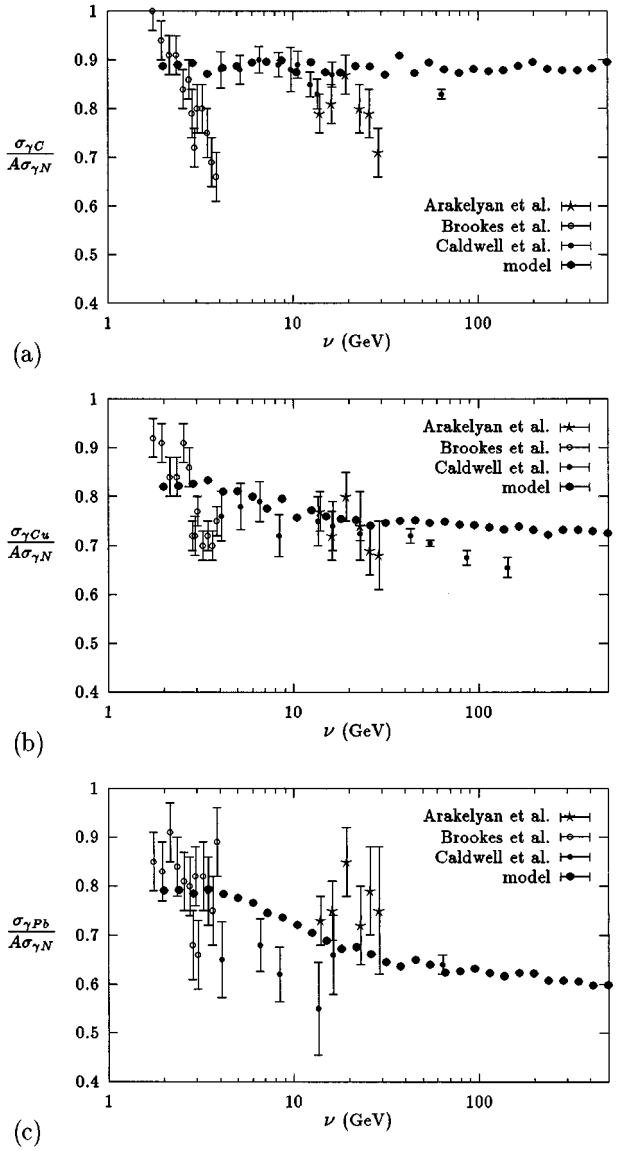

FIG. 6. Per-nucleon ratios of real photon-carbon (a), -copper (b), and -lead (c) cross sections to photon-nucleon cross sections are shown together with measurements [53–56].

As discussed initially, in direct photon interactions the Glauber multiple scattering process is, per definition, completely suppressed since the photon couples directly to a parton in a nucleon without leaving any remnant. In contrast, the assumption that also in anomalous photon interactions the Glauber cascade is reduced to one $q\bar{q}$-nucleon scattering can only be considered as an extreme case. In general, there is a leading-twist soft contribution to hard processes which, as discussed in [52], might influence the shadowing behavior even for large values of M^2. However, our assumption to neglect all shadowing contributions in direct and anomalous interactions is justified since we are interested in estimating the maximum possible effect of the pointlike interactions on the shadowing behavior at high energies. It is obvious how the pointlike processes have to be taken into account in Eq. (13): σ_{VN} has to be replaced by $(1-\xi)\sigma_{VN}$ and $A \cdot \sigma^{\mathrm{pl}}_{\gamma^* N}$ is added explicitly to Eq. (10), with

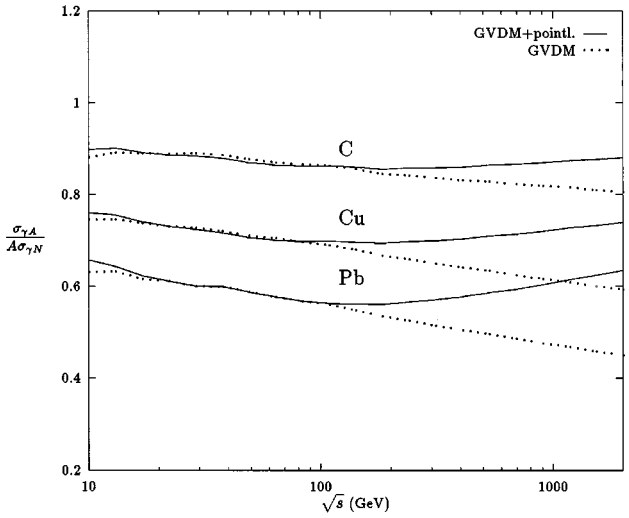

FIG. 7. As in Fig. 5 but for the shadowing ratios.

$$\xi(s,Q^2)=\frac{\sigma^{\rm pl}_{\gamma^\star N}(s,Q^2)}{\sigma^{\rm tot}_{\gamma^\star N}(s,Q^2)},$$

$$\sigma^{\rm pl}_{\gamma^\star N}(s,Q^2)=\sigma^{\rm dir}_{\gamma^\star N}(s,Q^2)+\sigma^{\rm ano}_{\gamma^\star N}(s,Q^2). \qquad (19)$$

In Fig. 4 we compare our results on $\sigma_{\gamma A}$ in the photoproduction limit ($Q^2=0$) for carbon, copper, and lead targets (solid lines) to data [53–56]. The agreement is reasonable apart from the low energy region where our results for the carbon target seem to show less shadowing than measured. However, for $\nu\approx 2-3$ GeV the lower energy limit of the applicability of the model is reached. In addition, we indicate with dotted lines the cross sections which would be obtained if one neglects the limited coherence length at low energies. Whereas this effect is less significant for light targets, it is responsible for the increase of the cross sections towards lower energies observed in interactions of real photons with copper and lead nuclei.

An extrapolation in energy of the real photon-nucleus cross section is presented in Fig. 5, again, for the three target nuclei carbon, copper, and lead. Here, the pointlike interactions lead to a stronger increase of the cross sections above a photon-nucleon c.m. energy of 100 GeV (solid lines) than it would be obtained neglecting the suppression of the Glauber-cascade by pointlike processes (dotted lines).

B. Nuclear shadowing of photons

The ratio of the total photon-nucleus to the total photon-nucleon cross section, which gives the effective number of nucleons $A_{\rm eff}$ ''seen'' by the photon projectile, has been measured in photoproduction experiments using carbon, copper, and lead targets [53–56]. We compare these data in the form $A_{\rm eff}/A$, frequently called ''effective attenuation,'' to results of our calculations in Fig. 6(a)–6(c). The agreement is reasonable. However, there are considerable uncertainties within the measurements as well as differences between the results obtained in different experiments which make it difficult to draw further conclusions from this comparison.

In Fig. 7 the shadowing ratios $\sigma_{\gamma^\star A}/(A\sigma_{\gamma^\star N})$ for real photons are extrapolated in energy up to a photon-nucleon c.m. energy of 2 TeV. In order to study the influence of pointlike processes to the high energy shadowing behavior we plot the full model (solid lines) and the cross sections obtained if the pointlike processes are not taken into consideration (dotted lines). From this comparison we conclude that pointlike processes are responsible for a decrease of the nuclear shadowing with increasing energy.

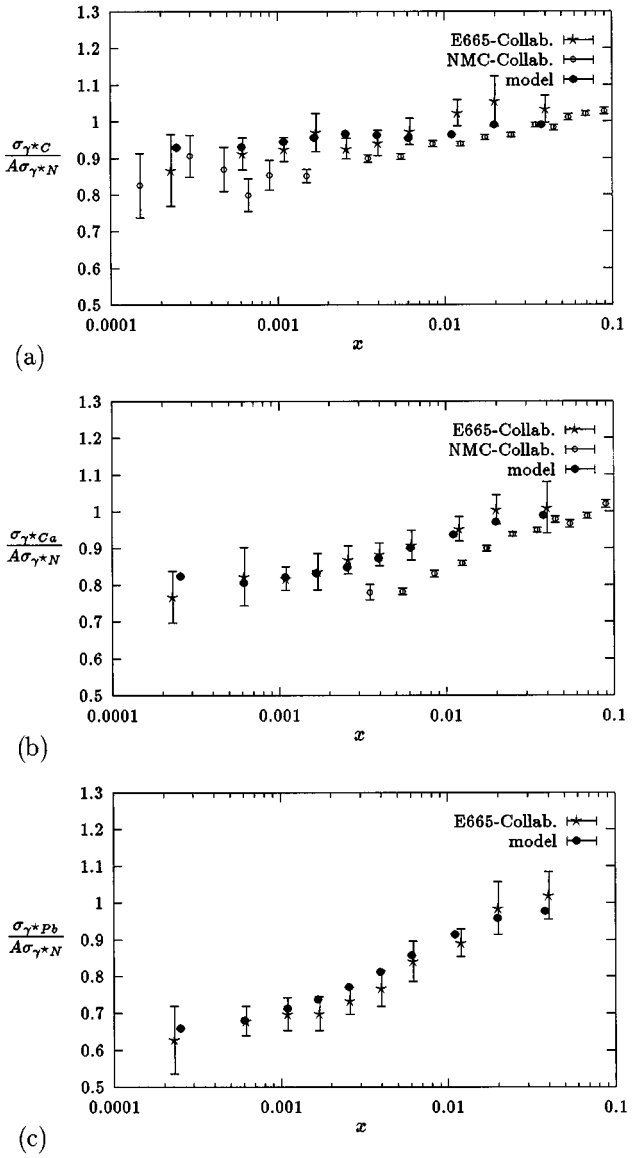

FIG. 8. The dependence of the per-nucleon ratios of photon-carbon (a), -calcium (b), and -lead (c) cross sections to photon-nucleon cross sections on the Bjorken-x is compared to data of the E665- [57] and NMC-Collaborations [58,59].

Let us now turn to lepton-nucleus interactions where the shadowing region ($x<0.1$) has been investigated by the E665 Collaboration using 470 GeV/c muons and by the New Muon Collaboration (NMC) using 200 GeV muons. Within our calculations the flux g of virtual photons is sampled according to the equivalent photon approximation (EPA) folded with the Q^2 dependent cross section $\sigma_{\gamma^\star A}$ [Eq. (10), see also [32] for details]

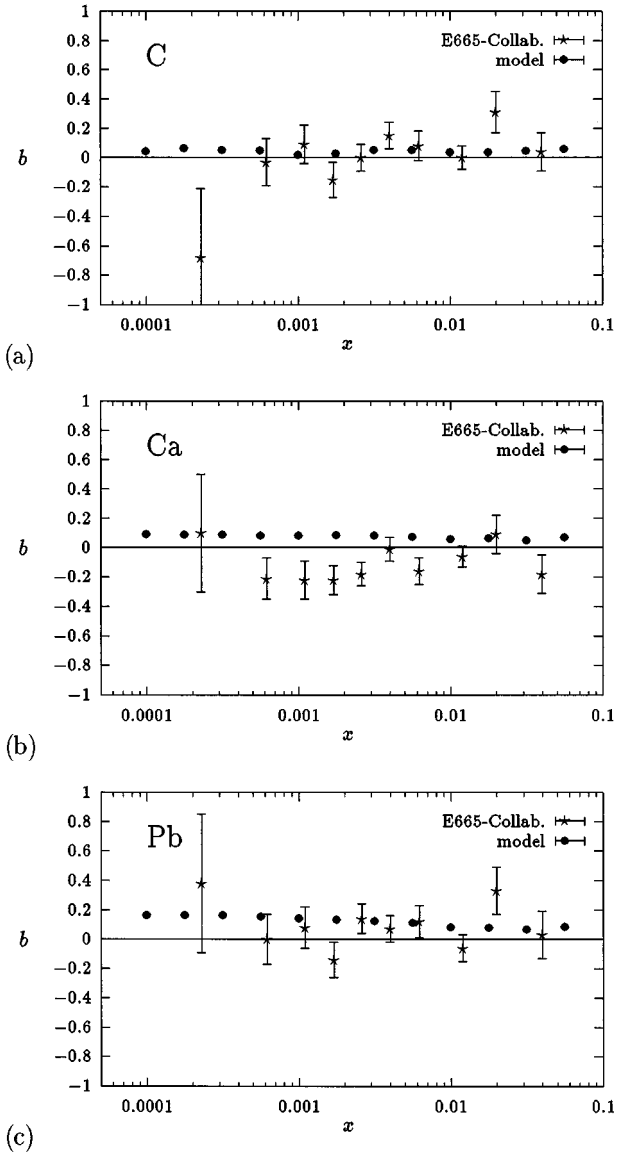

FIG. 9. The slopes of the logarithmic Q^2 dependence of the shadowing ratio R^A are compared to results of the E665 Collaboration [57].

$$\sigma_{lA}=\int dy \int dQ^2 g(y,Q^2)\sigma_{\gamma^\star A}(s,Q^2), \tag{20}$$

with y being the lepton energy fraction taken by the photon. The kinematic cuts as they were applied to the measured data are taken into account. In Fig. 8(a)–8(c) we compare the model predictions concerning the x dependence of the cross section ratios to E665 [57] and NMC data [58,59]. Our results are binned in the same way as the E665 data, showing that our photon-flux approximation gives average x values in each bin which correspond to the measured ones. The average Q^2 values range from 0.15 GeV^2 in the lowest x bin up to 7.9 GeV^2 in the highest bin. The calculations for the three target nuclei carbon, calcium, and lead are in reasonable agreement with the E665 data but overestimate the NMC data slightly.

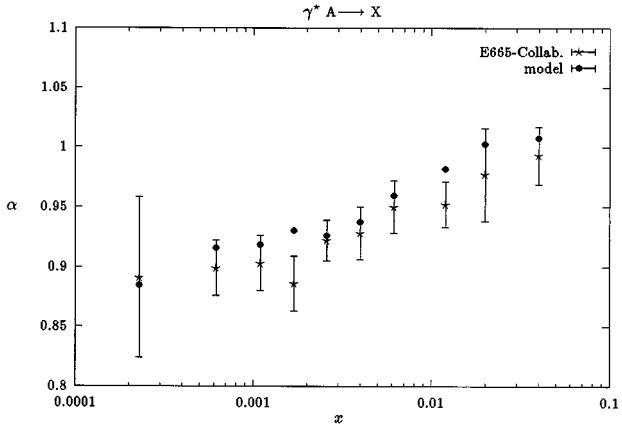

FIG. 10. The A dependence of the per-nucleon cross section ratios $R^A \propto A^{\alpha-1}$ for different bins of the Bjorken-x is shown together with E665 data [57].

In order to study the Q^2 dependence of the cross section ratios at fixed values of x we parametrize them as

$$R^A=\frac{\sigma_{\gamma^\star A}}{A\sigma_{\gamma^\star N}}=a+b\log_{10}(Q^2/\mathrm{GeV}^2). \tag{21}$$

In Fig. 9 we plot the slope b as function of x, again for carbon, calcium, and lead targets, together with E665 measurements [57]. Our results are consistent with the experimental observations, i.e., with a weak Q^2 dependence of the shadowing effect within the considered x range.

The strength of shadowing may also be studied by parametrizing the per-nucleon cross section ratios by $R^A \propto A^{\alpha-1}$. In Fig. 10 we compare results of our calculations on the values of α to E665 data [57]. Even though our values are systematically above the data, they are still compatible with them.

Extrapolating the shadowing ratios to high energies at fixed large values of Q^2 ($x\to 0$) Kopeliovich and Povh predicted within their model that shadowing vanishes [60]. As shown in Fig. 11 for carbon (a) and lead targets (b), within our model we predict the same qualitative features since the soft contributions are more strongly suppressed with the photon virtuality than the pointlike contributions. Applying an energy-independent cutoff to calculate the pointlike photon interactions, one would get also a decrease of shadowing in the photoproduction limit at very high energies. However, it is expected that the transverse momentum cutoff should increase with energy in order to guarantee that the calculation is restricted to a kinematic region where lowest-order perturbative QCD estimates are reliable. Several parametrizations of the energy dependence of the cutoff have been suggested in [61,62]. These parametrizations predict a only slowly varying cutoff up to c.m. energies of about 2 TeV. Therefore, we assume that the qualitative results reported here do not change applying an energy-dependent cutoff. This has been confirmed numerically for the parametrization discussed in [62].

C. Quasielastic vector meson production

A further test of the Q^2 behavior of our model can be performed by studying quasielastic vector meson production.

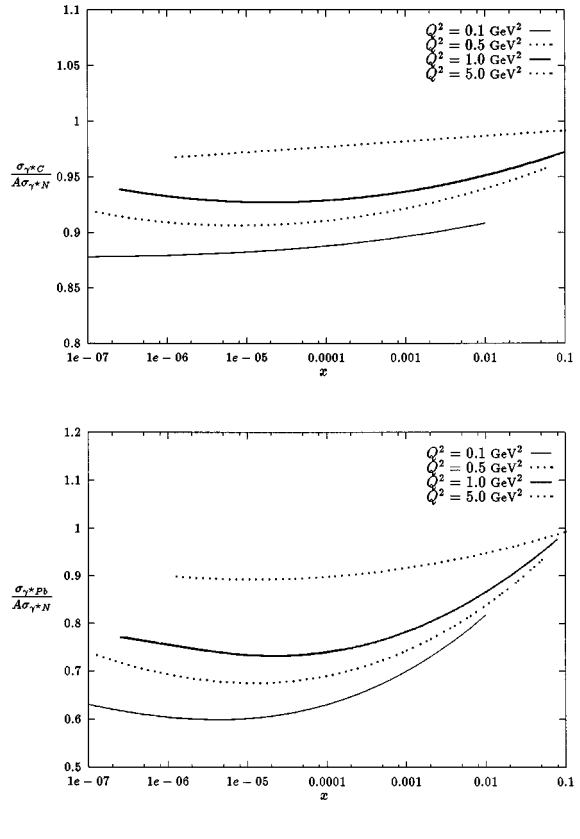

FIG. 11. Bjorken-x-dependence of the per-nucleon ratios of photon-carbon (a) and photon-lead (b) cross sections to photon-nucleon cross sections shown for $Q^2=0.1$, 0.5, 1.0, and 5.0 GeV^2 (from the bottom to the top).

For example, the cross section for the (coherent) quasielastic ρ^0 production off a nucleus with mass number A depends on Q^2 like

$$\sigma_{\gamma^* A\to\rho^0 A}(s,Q^2)\sim\left(\frac{m_\rho^2}{m_\rho^2+Q^2}\right)^2\left(1+\epsilon\frac{Q^2}{m_\rho^2}\right)\sigma^{\rm el}_{\rho^0 A}(s,Q^2), \tag{22}$$

where $\sigma^{\rm el}_{\rho^0 A}$ is obtained according to Eq. (18). In Fig. 12 we show our results together with data of the NMC Collaboration [63]. In each Q^2 bin, the average photon energy and the average value of ϵ were used as given in [63]. In order to compare the shape, our results were normalized to the data. Parametrizing $\sigma^{\rm el}_{\rho^0 A}$ as

$$\sigma^{\rm el}_{\rho^0 A}(Q^2)=\sigma_0\left(\frac{Q_0^2}{Q^2}\right)^\beta \tag{23}$$

we get from a fit to our results values for β of 2.6 for deuterium, 2.5 for carbon, and 2.4 for calcium. Since our results slightly deviate from a power-law behavior in Q^2 we estimate the uncertainties for the β values by excluding either the cross sections at the two lowest or highest Q^2 from the fit. For the three β values we obtain an uncertainty of ± 0.2. Comparing it to the experimental value of $\beta=2.02\pm 0.07$ from a combined fit to the data for the three

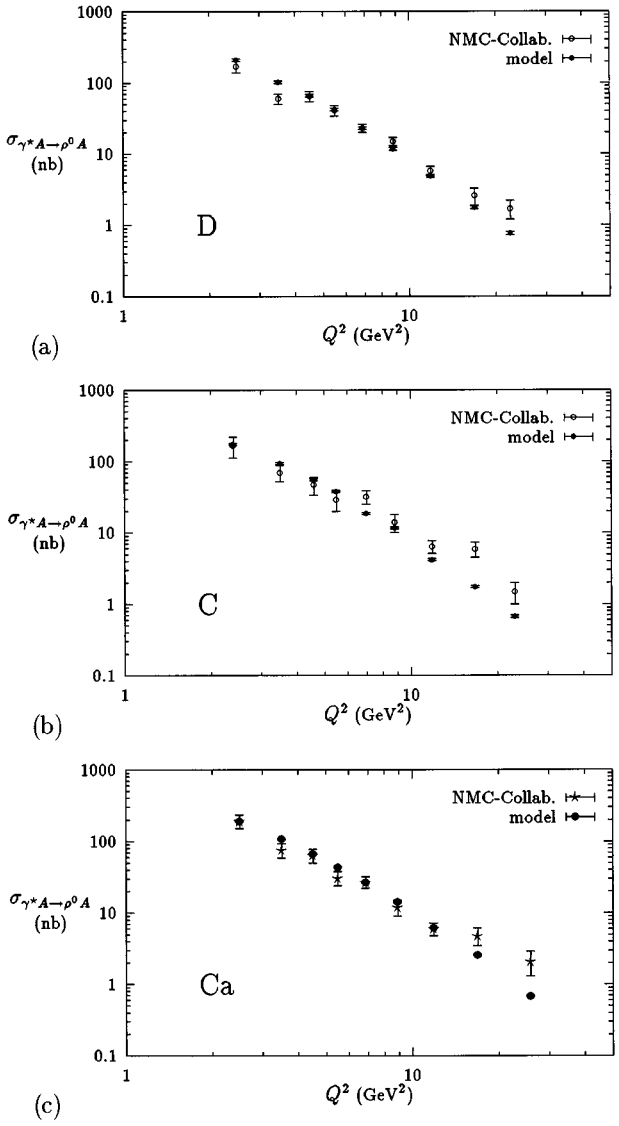

FIG. 12. Dependence of the quasielastic ρ^0-production cross sections on the photon virtuality for photon-deuterium (a), -carbon (b), and -calcium (c) interactions. The model results are normalized to the data of the NMC Collaboration [63].

target nuclei [63], we conclude that our results show a somewhat stronger Q^2 dependence than the NMC data. This deviation might be caused by the fact that we do not explicitly treat the ρ, ω, and ϕ vector mesons but instead include them into the mass continuum Eq. (1). Considering the low-mass vector mesons separately in Eq. (1) we would expect a better agreement between the quasielastic ρ production data and the model. However, in this case new parameters would be introduced into the model which are not needed for the investigation of the influence of pointlike effects on shadowing. Furthermore, we note that the values of the kinematic variables s and Q^2 of the experiment partially exceed the limit $Q^2\ll s$ where our simple approach can be expected to be reliable.

V. SUMMARY AND CONCLUSIONS

Cross sections for photon-nucleus interactions are calculated based on the assumption that the photon may interact

directly or as a ''resolved'' $q\bar{q}$ state. We apply the generalized vector dominance model together with Glauber-Gribov theory taking coherence length effects into account. Total photon-nucleon cross sections are calculated within the CKMT model.

We assume that direct and anomalous photon interactions are pointlike, i.e., the photon interacts with only one target nucleon. The cross sections corresponding to the pointlike processes are estimated within lowest order perturbative QCD. The suppression of the Glauber cascade due to these pointlike photon interactions is explicitly taken into account.

Real photon-nucleus cross sections are compared to data and extrapolated to high energies. In addition, we study the shadowing behavior in photon-nucleus interactions for moderate photon virtualities by comparing them to data. In both cases a reasonable agreement with the data is found. It is discussed that pointlike photon interactions lead to a suppressed shadowing in interactions with heavy target nuclei at high energies.

In [24] this study is extended to particle production in interactions of weakly virtual photons off nuclei. There, the description of particle production is based on the above discussed cross sections and shadowing behavior combined with the ideas of the two-component dual parton model describing photon-nucleon interactions.

ACKNOWLEDGMENTS

Discussions with F. W. Bopp are gratefully acknowledged. One of the authors (J.R.) thanks C. Pajares for the hospitality at the University Santiago de Compostela, and he was supported by the Direccion General de Politicia Cientifica of Spain. One of the authors (R.E.) was supported by the Deutsche Forschungsgemeinschaft under Contract No. Schi 422/1-2.

[1] M. Erdmann, ''The Partonic Structure of the Photon: Photoproduction at the Lepton-Proton Collider HERA,'' Report No. DESY 96-090, 1996 (unpublished).
[2] AMY Collaboration, R. Tanaka *et al.*, Phys. Lett. B **277**, 215 (1992).
[3] H1 Collaboration, T. Ahmed *et al.*, Phys. Lett. B **297**, 205 (1992).
[4] ZEUS Collaboration, M. Derrick *et al.*, Phys. Lett. B **322**, 287 (1994).
[5] H1 Collaboration, S. Aid *et al.*, Z. Phys. C **70**, 17 (1995).
[6] ZEUS Collaboration, M. Derrick *et al.*, Phys. Lett. B **354**, 136 (1995).
[7] M. Drees and R. M. Godbole, Pramana, J. Phys. **41**, 83 (1993).
[8] M. Drees and R. M. Godbole, J. Phys. G **21**, 1559 (1995).
[9] T. H. Bauer, R. D. Spital, and D. R. Yennie, Rev. Mod. Phys. **50**, 261 (1978).
[10] G. Grammer, Jr. and D. Sullivan, in *Electromagnetic Interactions of Hadrons*, edited by A. Donnachie and G. Shaw (Plenum Press, New York, 1978), Vol. 2.
[11] J. F. Owens, Phys. Rev. D **21**, 54 (1980).
[12] E. Witten, Nucl. Phys. **B120**, 189 (1977).
[13] M. Arneodo, Phys. Rep. **240**, 301 (1994).
[14] G. Piller, W. Ratzka, and W. Weise, Z. Phys. A **352**, 427 (1995).
[15] A. Donnachie and G. Shaw, in *Electromagnetic Interactions of Hadrons* [10], Vol. 2.
[16] R. J. Glauber, Phys. Rev. **100**, 242 (1955).
[17] V. N. Gribov, Sov. Phys. JETP **30**, 709 (1970).
[18] L. Bertochi, Nuovo Cimento A **11**, 45 (1972).
[19] L. L. Frankfurt and M. I. Strikman, Nucl. Phys. **B316**, 340 (1989).
[20] L. L. Frankfurt, G. A. Miller, and M. I. Strikman, Annu. Rev. Nucl. Part. Sci. **45**, 501 (1994).
[21] G. V. Davidenko and N. N. Nikolaev, Nucl. Phys. **B135**, 333 (1978).
[22] B. L. Ioffe, V. A. Khoze, and L. N. Lipatov, *Hard Processes, Volume 1: Phenomenology Quark-Parton Model* (North-Holland, Amsterdam, 1984).
[23] J. Hüfner, B. Kopeliovich, and J. Nemchik, Phys. Lett. B **383**, 362 (1996).
[24] S. Roesler, R. Engel, and J. Ranft, ''Photoproduction off nuclei and point-like photon interactions, Part II: Particle production,'' Report No. SI 96-14, US-FT/45-96, hep-ph/9611379, 1996 (unpublished).
[25] J. J. Sakurai and D. Schildknecht, Phys. Lett. **40B**, 121 (1972).
[26] B. Gorczyca and D. Schildknecht, Phys. Lett. **47B**, 71 (1973).
[27] V. M. Budnev, I. F. Ginzburg, G. V. Meledin, and V. G. Serbo, Phys. Rep., Phys. Lett. **15C**, 181 (1975).
[28] A. Capella, A. Kaidalov, C. Merino, and J. Trân Thanh Vân, Phys. Lett. B **337**, 358 (1994).
[29] H. Abramowicz, E. M. Levin, A. Levy, and U. Maor, Phys. Lett. B **269**, 465 (1991).
[30] B. Badelek and J. Kwieciński, Phys. Lett. B **295**, 263 (1992).
[31] R. Engel, Z. Phys. C **66**, 203 (1995).
[32] R. Engel and J. Ranft, Phys. Rev. D **54**, 4244 (1996).
[33] S. I. Alekhin, ''Compilation of cross sections 4,'' CERN-HERA Report No. 87-01, 1987 (unpublished).
[34] ZEUS Collaboration, M. Derrick *et al.*, Z. Phys. C **63**, 391 (1994).
[35] H1 Collaboration, S. Aid *et al.*, Z. Phys. C **69**, 27 (1995).
[36] H. Abramowicz, K. Charchula, M. Krawczyk, A. Levy, and U. Maor, Int. J. Mod. Phys. A **8**, 1005 (1993).
[37] T. Sjöstrand, Phys. Lett. **157B**, 321 (1985).
[38] T. Gottschalk, Nucl. Phys. **B277**, 700 (1986).
[39] M. Glück, E. Reya, and A. Vogt, Z. Phys. C **53**, 127 (1992).
[40] H1 Collaboration, S. Aid *et al.*, Nucl. Phys. **B470**, 3 (1996).
[41] ZEUS Collaboration, M. Derrick *et al.*, Z. Phys. C **72**, 399 (1996).
[42] CTEQ-Collaboration, H. L. Lai *et al.*, Phys. Rev. D **55**, 1280 (1997).
[43] A. D. Martin, R. G. Roberts, and W. J. Stirling, Phys. Lett. B **387**, 419 (1996).
[44] M. Glück, E. Reya, and A. Vogt, Phys. Rev. D **46**, 1973 (1992).
[45] M. Glück, E. Reya, and A. Vogt, Phys. Rev. D **45**, 3986 (1992).
[46] H1 Collaboration, T. Ahmed *et al.*, Nucl. Phys. **B445**, 195 (1995).
[47] G. A. Schuler and T. Sjöstrand, Z. Phys. C **68**, 607 (1995).

[48] J. Kwieciński, Phys. Lett. B **184**, 386 (1987).
[49] S. Y. Shmakov, V. V. Uzhinskii, and A. M. Zadoroshny, Comput. Phys. Commun. **54**, 125 (1989).
[50] L. P. A. Haakman, A. Kaidalov, and J. H. Koch, Phys. Lett. B **365**, 411 (1996).
[51] E. Segré, *Nuclei and Particles* (Benjamin, Reading, MA, 1977).
[52] B. Kopeliovich, in *Proceedings of the Workshop Hirschegg'95: Dynamical Properties of Hadrons in Nuclear Matter*, edited by H. Feldmeier and W. Nörenberg (GSI, Darmstadt, 1996), p. 102.
[53] E. A. Arakelyan *et al.*, Phys. Lett. **79B**, 143 (1978).
[54] G. R. Brookes *et al.*, Phys. Rev. D **8**, 2826 (1973).
[55] D. O. Caldwell *et al.*, Phys. Rev. D **7**, 1362 (1973).
[56] D. O. Caldwell *et al.*, Phys. Rev. Lett. **42**, 553 (1979).
[57] E665 Collaboration, M. R. Adams *et al.*, Z. Phys. C **67**, 403 (1995).
[58] New Muon Collaboration, P. Amaudruz *et al.*, Z. Phys. C **51**, 387 (1991).
[59] New Muon Collaboration, M. Arneodo *et al.*, Nucl. Phys. **B441**, 12 (1995).
[60] B. Kopeliovich and B. Povh, Z. Phys. A **356**, 467 (1997).
[61] K. Geiger, Phys. Rev. D **47**, 133 (1993).
[62] F. W. Bopp, R. Engel, D. Pertermann, and J. Ranft, Phys. Rev. D **49**, 3236 (1994).
[63] New Muon Collaboration, M. Arneodo *et al.*, Nucl. Phys. **B429**, 503 (1994).